

LAPTOP-Diff: Layer Pruning and Normalized Distillation for Compressing Diffusion Models

Dingkun Zhang*
OPPO AI Center
Shenzhen, China
zhangdingkun@oppo.com

Sijia Li*
OPPO AI Center
Shenzhen, China
lisijia@oppo.com

Chen Chen†
OPPO AI Center
Shenzhen, China
chenchen4@oppo.com

Qingsong Xie
OPPO AI Center
Shenzhen, China
xieqingsong1@oppo.com

Haonan Lu†
OPPO AI Center
Shenzhen, China
luhaonan@oppo.com

Images generated with the original 2.6B U-Net



Images generated with our pruned 1.3B U-Net



Figure 1: Visual comparison between the original model and our 50% pruned model. Our 1.3B U-Net is pruned and retrained from ZavychromaXL-v1.0.

ABSTRACT

In the era of AIGC, the demand for low-budget or even on-device applications of diffusion models emerged. In terms of compressing the Stable Diffusion models (SDMs), several approaches have been proposed, and most of them leveraged the handcrafted layer removal methods to obtain smaller U-Nets, along with knowledge distillation to recover the network performance. However, such a handcrafting manner of layer removal is inefficient and lacks scalability and generalization, and the feature distillation employed in the retraining phase faces an imbalance issue that a few numerically significant feature loss terms dominate over others throughout the retraining process. To this end, we proposed the layer pruning and normalized distillation for compressing diffusion models (LAPTOP-Diff). We, 1) introduced the layer pruning method to compress

SDM’s U-Net automatically and proposed an effective one-shot pruning criterion whose one-shot performance is guaranteed by its good additivity property, surpassing other layer pruning and handcrafted layer removal methods, 2) proposed the normalized feature distillation for retraining, alleviated the imbalance issue. Using the proposed LAPTOP-Diff, we compressed the U-Nets of SDXL and SDM-v1.5 for the most advanced performance, achieving a minimal 4.0% decline in PickScore at a pruning ratio of 50% while the comparative methods’ minimal PickScore decline is 8.2%. We will release our code.

1 INTRODUCTION

Generative modeling for text-to-image (T2I) synthesis has experienced rapid progress in recent years. Especially, the diffusion model[6, 13, 28, 31, 46] emerged with its capability of generating high-resolution, photorealistic, and diverse images. Among all the diffusion models, Stable Diffusion model (SDM)[28, 31] is the most

*Equal contribution.

†Corresponding author.

influential one, playing a pivotal role in the AIGC community as an open-source framework, serving as the foundation of a wide spectrum of downstream applications.

However, SDM’s remarkable performance comes with its considerable memory consumption and latency, making its deployment on personal computers or even mobile devices highly constrained. Furthermore, recent versions of the SDM series, e.g., SDXL[28], tend to grow larger in parameters, resulting in even greater memory consumption and latency. To reduce the SDM’s inference budget, several approaches have been proposed, i.e., denoising step reduction[22, 25, 35, 37, 53], efficient architecture designing[9, 16, 19, 55], structural pruning[8], quantization[21, 43], and hardware-aware optimization[5]. These approaches are generally orthogonal to each other.

Among these approaches, efficient architecture designing and structural pruning are understudied. On the one hand, the previous efficient architecture designing approaches[9, 16, 19, 55] typically go through substantial empirical studies to identify the unimportant layers of SDM’s U-Net and then remove them to achieve a smaller and faster network. Such a handcrafting manner usually can not achieve the best performance and lacks scalability and generalization. We noticed that these hand-crafted layer-removal methods can be substituted by the layer-pruning method in an automatic scheme for better scalability and performance. On the other hand, the previous structural pruning approach[8] on SDM focused on the fine-grained pruning, i.e., pruning rows and columns of parameter matrices. However, there are studies[7, 15] suggest that the fine-grained pruning is generally less efficient in reducing model latency compared to the coarser-gained layer pruning, and interestingly, layer pruning is possible to achieve the same performance as finer-gained structural pruning or even better. Based on the above two points, the layer pruning method is worth studying.

After the layer removal or pruning, the SDMs often cannot generate clear images directly. Previous methods[9, 16, 19, 55] exploit knowledge distillation to retrain the pruned network to recover its performance. Previous methods typically leveraged three types of objectives, i.e., regular training objective, logit distillation(output distillation)[12] objective, and feature distillation[33] objective. Among the three parts, feature distillation is the pivotal one. However, our further examinations revealed an imbalance issue in the previous distillation-based retraining method that a few feature loss terms dominated over others throughout the retraining process, leading to degraded performance.

In this work, we proposed the LAYER Pruning and normalized distillation for cOmpressing Diffusion models(LAPTOP-Diff), pushing the realms of efficient architecture designing and structural pruning for SDM toward automation, scalability, and greater performance. We formulated the problem of layer pruning from a high perspective of the combinatorial optimization problem and solved it in a simple yet effective one-shot manner. Benefiting from such perspective, we explored several other possible pruning criteria, and through ablation studies, we were able to discover that the effectiveness of our one-shot layer pruning criterion comes from its good additivity property[47, 52]. Further, we identified an imbalance issue in the previous distillation-based retraining method that a few feature

loss terms dominated over others throughout the retraining process, and we alleviated this issue through the proposed normalized feature distillation. Our contributions are summarized as follows:

- We explored layer pruning, an understudied approach of structural pruning, on SDMs, and proposed an effective one-shot pruning criterion whose one-shot performance is guaranteed by its good additivity property, surpassing other layer pruning and handcrafted layer removal methods, pushing the previous layer-remove-based efficient architecture designing approaches toward automation, scalability, and greater performance.
- We alleviated the imbalance issue of the previous distillation-based retraining using the proposed normalized feature distillation.
- Our proposed LAPTOP-Diff greatly surpasses the layer-remove-based efficient architecture designing approaches in terms of network performance across different SDMs and pruning ratios.

2 RELATED WORK

2.1 Diffusion Model

Diffusion model[6, 13, 28, 31, 46] is a type of generative model that leverages iterative denoising process to synthesize data. In the realm of text-to-image(T2I) synthesis, the diffusion models such as DALL·E[30], Imagen[34], Deepfloyd IF[1], and Stable Diffusion[31] demonstrated their remarkable capability of generating high-resolution, photo-realistic, and diverse images. Among various diffusion models, Stable Diffusion[31] is the most influential one in both the academic community and the industry. Stable Diffusion model(SDM) is a type of Latent Diffusion model that performs the iterative denoising process in the low-dimensional latent space and then transforms the latent representations into pixel-space images through a VAE decoder. There is also a more recent version of the SDM series, i.e., SDXL[28], which demonstrates superior image generation quality at a higher resolution of 1024×1024.

However, the impressive performance of diffusion models comes with substantial memory consumption and latency. To reduce the model budget of SDM, several approaches have been explored, e.g., denoising step reduction[22, 25, 35, 37, 53], quantization[21, 43], hardware-aware optimization[5], efficient architecture designing[9, 16, 19, 55], and structural pruning[8].

2.2 Efficient Architecture Designing for SDM

Orthogonal to many other approaches of reducing SDM’s model budget, efficient architecture designing mainly aims to design an efficient sub-structure of the original SDM’s U-Net since most of the SDM’s memory consumption and latency comes from its U-Net. Previous methods[9, 16, 19, 55] of this kind typically go through substantial empirical studies to identify the unimportant layers of the SDM’s U-Net and remove them to achieve a smaller and faster network. BK-SDM[16] handcrafted 3 efficient U-Nets of different sizes for SDM-v1 or SDM-v2 by layer removal, partially following the empirical conclusion of DistilBERT[36] which is an empirical work on compressing the BERT model. SSD-1B[9] and Segmind-Vega[9] (we refer to them as SSD and Vega for the rest of this paper) handcrafted 2 efficient U-Nets of different sizes for SDXL by

identifying the unimportant layers through human evaluation and then imposing layer removal. KOALA[19] is derived from BK-SDM and handcrafted 2 efficient U-Nets of different sizes for SDXL also by layer removal.

Such a handcrafting manner usually can not achieve the best performance and lacks scalability and generalization. We noticed that these layer-remove-based methods can be categorized as handcrafted layer pruning. Hence, we propose that these handcrafted layer-remove methods can be substituted by the layer pruning method in an automatic scheme for better scalability and performance.

2.3 Layer Pruning

Layer pruning[4, 7, 15], also known as depth pruning, is a type of structural pruning method that aims to automatically evaluate and remove unimportant layers. Unlike other structural pruning methods, layer pruning is paid little attention due to its coarse-grained nature. Layer pruning is often considered less effective compared to those fine-grained structural pruning methods. However, there are studies[7, 15] showed that, compared to fine-grained structural pruning methods, coarse-grained layer pruning is generally more efficient in reducing model’s latency and possible to achieve the same performance or even better.

Although there are several layer pruning methods[4, 7, 15] have been proposed, none of which viewed layer pruning through a combinatorial optimization problem perspective. Magnitude-based and Taylor-expansion-based pruning are common baselines. Magnitude-based layer pruning uses the summed magnitude of the parameters in a layer as the layer importance criterion, and Taylor-expansion-based layer pruning uses the first-order Taylor-expansion of the loss function as the layer importance criterion. After evaluating the importance of each layer by different importance criteria, the previous layer pruning methods then opt to prune the least important layers.

In this work, we formulated the problem of layer pruning from a higher perspective of the combinatorial optimization problem and solved it in a simple yet effective one-shot manner, forming an effective one-shot pruning criterion, surpassing other layer pruning and handcrafted layer removal methods. Furthermore, through such a perspective, we were able to identify that the effectiveness of our one-shot layer pruning criterion comes from its good additivity property[47, 52].

2.4 Distillation-Based Retraining

After the layer removal or pruning, the SDMs often can not generate clear images directly. Previous methods[9, 16, 19, 55] retrain the pruned SDMs by utilizing knowledge distillation to recover their performance. Knowledge distillation used in the retraining phase usually consists of three parts, i.e., regular training objective, logit distillation(output distillation)[12], and feature distillation[33]. Among the three parts, feature distillation is the most effective one.

However, in practice, we located an imbalance issue in the distillation-based retraining process. To this end, we proposed a simple yet effective re-weighting strategy to alleviate this issue.

3 METHODOLOGY

3.1 Preliminary

The SDM’s U-Net can be viewed as a stack of residual layers, transformer layers, and several up/down sampling convolutional layers, omitting the skip connections. The majority of these layers are consistent in the shape of their own inputs and outputs. Thus, these layers can be removed directly without causing a shape mismatch problem. Specifically, except for several residual layers that involve alterations of the number of input and output channels, all the residual layers and transformer layers of SDM’s U-Net are prunable as shown in Fig. 2. The prunable layers account for 88% and 98% total parameters of the entire U-Net of SDM-v1.5 and SDXL respectively. We denote the collection of all the n prunable layers as $L^n = \{l_1, \dots, l_n\}$ where l_i is a single residual layer or transformer layer.

The previous approaches[9, 16] of retraining the pruned SDM’s U-Net leverage three objectives, i.e., task loss, output distillation[12] loss and feature distillation[33] loss:

$$\begin{aligned} \mathcal{L}_{Task} &= \mathbb{E}_{z,y,t,\epsilon} \|\epsilon - \epsilon_S(z_t, y, t)\|_2^2, \\ \mathcal{L}_{OutKD} &= \mathbb{E}_{z,y,t} \|\epsilon_T(z_t, y, t) - \epsilon_S(z_t, y, t)\|_2^2, \\ \mathcal{L}_{FeatKD} &= \sum_i \mathbb{E}_{z,y,t} \|f_T^i(z_t, y, t) - f_S^i(z_t, y, t)\|_2^2, \end{aligned} \quad (1)$$

where z, y and $t \sim Uniform(0, T)$ denote the latent representation, its corresponding condition, and its corresponding time step. $\epsilon \sim N(0, I)$ denote the ground-truth noise. ϵ_S and ϵ_T are the outputs of the student and the teacher where the student is the pruned U-Net and the teacher is the frozen original U-Net. f_T^i and f_S^i represent the feature maps at the end of the i -th stage in the teacher and the student, respectively. We refer to the $\mathbb{E}_{z,y,t} \|f_T^i(z_t, y, t) - f_S^i(z_t, y, t)\|_2^2$ terms for different i as feature loss terms in this paper. The \mathcal{L}_{OutKD} and \mathcal{L}_{FeatKD} are knowledge distillation objectives. The three objectives are also illustrated in Fig. 2. The overall objective is $\mathcal{L}_{all} = \mathcal{L}_{Task} + \lambda_{OutKD} \mathcal{L}_{OutKD} + \lambda_{FeatKD} \mathcal{L}_{FeatKD}$. Where the λ_{OutKD} and λ_{FeatKD} are hyperparameters, both of which are usually set to 1 as default.

3.2 One-Shot Layer Pruning

The goal of layer pruning is to remove a subset of prunable layers from the U-Net that satisfies a given pruning ratio while causing a minimal decrease in network performance. We opt to minimize the Mean-Squared-Error loss between the final outputs of the original network and the pruned network given a pruning ratio. There are also other possible objectives, and we will discuss them at the end of this section. Let ϵ_{ori} denote the output of the original network, $r_i \in L^n$ denote the i -th removed layer, and $\epsilon(r_1, r_2, \dots, r_m)$ denote the output of the network where the layers r_1, r_2, \dots, r_m are removed. Notice that the m is an undetermined variable. The optimization problem is formulated as follows:

$$\begin{aligned} \min_{r_1, \dots, r_m} \quad & \mathbb{E} \|\epsilon(r_1, \dots, r_m) - \epsilon_{ori}\|_2^2 \\ \text{s.t.} \quad & \{r_1, \dots, r_m\} \subset L^n, \sum_{i=1}^m \text{params}(r_i) \geq P, \end{aligned} \quad (2)$$

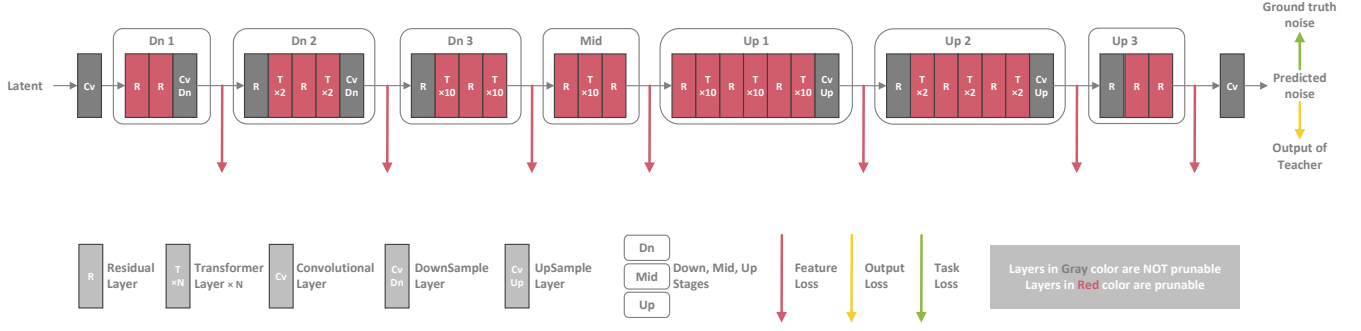


Figure 2: Architecture of SDM’s U-Net and knowledge distillation framework, using SDXL as an example. Other SDMs’ U-Net have slightly different architectures, e.g., SDM-v1.5 has 4 Dn and Up stages instead of 3 and has fewer transformer layers.

where the $param(r_i)$ denotes the total count of parameters of layer r_i , and P is the number of parameters to prune which is calculated by the total number of parameters of the original network multiplied by the pruning ratio. Directly solving this optimization problem requires the search on all combinations of $\{r_1, r_2, \dots, r_m\}$ which is NP-hard. Therefore, we try to find a surrogate objective.

Upper bound of objective (2). According to the triangle inequality, we have an upper bound of formula (2):

$$\begin{aligned}
& \mathbb{E} \|\epsilon(r_1, \dots, r_m) - \epsilon_{ori}\|_2^2 \\
& \leq \mathbb{E} \|\epsilon(r_1) - \epsilon_{ori}\|_2^2 \\
& \quad + \mathbb{E} \|\epsilon(r_1, r_2) - \epsilon(r_1)\|_2^2 \\
& \quad + \dots \\
& \quad + \mathbb{E} \|\epsilon(r_1, \dots, r_m) - \epsilon(r_1, \dots, r_{m-1})\|_2^2.
\end{aligned} \tag{3}$$

Therefore, we find a surrogate objective for the objective (2):

$$\begin{aligned}
& \min_{r_1, \dots, r_m} \mathbb{E} \|\epsilon(r_1) - \epsilon_{ori}\|_2^2 + \mathbb{E} \|\epsilon(r_1, r_2) - \epsilon(r_1)\|_2^2 + \dots \\
& \quad + \mathbb{E} \|\epsilon(r_1, \dots, r_m) - \epsilon(r_1, \dots, r_{m-1})\|_2^2 \\
& \text{s.t. } \{r_1, \dots, r_m\} \subset L^n, \sum_{i=1}^m param(r_i) \geq P.
\end{aligned} \tag{4}$$

Solving the optimization problem (4) is still NP-hard. However, it led us to another, better surrogate objective.

Approximation of upper bound (4). We noticed that each term of the formula (4) is the Mean-Squared-Error loss between a network(pruned or unpruned) and the network where one additional layer is removed, e.g., $\|\epsilon(r_1, \dots, r_{i-1}, r_i) - \epsilon(r_1, \dots, r_{i-1})\|_2^2$ is the Mean-Squared-Error loss between the network where layers r_1, \dots, r_{i-1} are removed and the network where layers r_1, \dots, r_{i-1}, r_i are removed. We conjecture that the Mean-Squared-Error loss caused by removing the same layer r_i are similar across different networks. The assumption is formulated as follows:

$$\begin{aligned}
& \mathbb{E} \|\epsilon(r_1, \dots, r_{i-1}, r_i) - \epsilon(r_1, \dots, r_{i-1})\|_2^2 \\
& \approx \mathbb{E} \|\epsilon(r_1, \dots, r_{i-2}, r_i) - \epsilon(r_1, \dots, r_{i-2})\|_2^2 \\
& \approx \dots \\
& \approx \mathbb{E} \|\epsilon(r_1, r_i) - \epsilon(r_1)\|_2^2 \\
& \approx \mathbb{E} \|\epsilon(r_i) - \epsilon_{ori}\|_2^2.
\end{aligned} \tag{5}$$

Algorithm 1 One-Shot Layer Pruning

Input: A network with prunable layers $L^n = \{l_0, l_1, \dots, l_n\}$, a calibration dataset X , parameters of total quantity P to prune

Output: A set of layers to prune $R^m \subset L^n$

- 1: **for** l_i in L^n **do**
- 2: calculate $values[i] = \mathbb{E} \|\epsilon(l_i) - \epsilon_{ori}\|_2^2$ on dataset X
- 3: $weights[i] = param(l_i)$
- 4: **end for**
- 5: $knapsack_capacity = P$
- 6: acquires R^m by solving the variant 0-1 Knapsack problem (6) given $values, weights, knapsack_capacity$, using dynamic programming
- 7: **return** R^m

Finally with assumption (5), we can optimize the objective (4) by optimizing its approximated objective:

$$\begin{aligned}
& \min_{r_1, \dots, r_m} \sum_{i=1}^m \mathbb{E} \|\epsilon(r_i) - \epsilon_{ori}\|_2^2 \\
& \text{s.t. } \{r_1, \dots, r_m\} \subset L^n, \sum_{i=1}^m param(r_i) \geq P.
\end{aligned} \tag{6}$$

Using the objective (6) to surrogate the original objective (2) implies an interesting property called additivity[47, 52] that a network’s output distortion caused by many perturbations approximately equals to the sum of output distortion caused by each single perturbation. Further experiments in Sec 4.3 validated the additivity property of our method on SDMs, showing that the final objective (6) is an excellent approximation of the original objective (2), meanwhile, the assumption (5) is well supported.

Here, the term $\mathbb{E} \|\epsilon(r_i) - \epsilon_{ori}\|_2^2$ functions as a pruning criterion. We only need to compute $\mathbb{E} \|\epsilon(l_i) - \epsilon_{ori}\|_2^2$, i.e., the output loss between the original network and the network where only layer l_i is removed, for each layer $l_i \in L^n$ with the total time complexity of $O(n)$, then the optimization problem (6) becomes a variant of the 0-1 Knapsack problem. Similar to the original 0-1 Knapsack problem, this variant problem can also be solved by the dynamic programming algorithm or can be approximately solved by the greedy algorithm. Both pseudocodes are given in the supplementary. When using the greedy algorithm, the solution degenerates

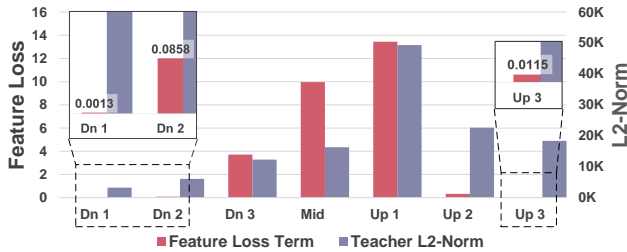


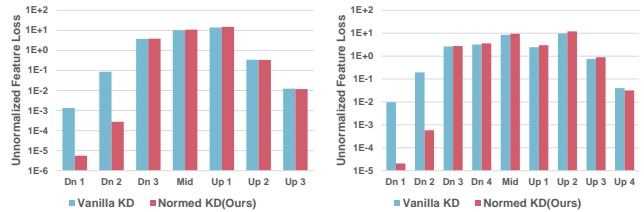
Figure 3: L2-Norms of feature maps at the end of each stage of the SDXL teacher and the feature loss terms at the 15K-th iteration of retraining.

to recurrently pruning the least important layer until the condition $\sum_{i=1}^m \text{params}(r_i) \geq P$ is satisfied, the same scheme as the previous approaches adopted. The greedy algorithm is simpler to implement, but the dynamic programming algorithm is always better. We used the dynamic programming algorithm in our work. Finally, the one-shot layer pruning method is summarized in Algorithm.1.

Discussions. In this section, we formulated the one-shot layer pruning problem as a combinatorial optimization problem and derived a pruning criterion, i.e., the output loss $\mathbb{E} \|\epsilon(l_i) - \epsilon_{ori}\|_2^2$. Furthermore, using the similar derivation form formula (2) to formula (6), we can construct some other possible pruning criteria, i.e., Δ task loss, Δ CLIP score[10], calculated by $\mathbb{E} |\mathcal{L}(r_i) - \mathcal{L}_{ori}|$ and $\mathbb{E} |C(r_i) - C_{ori}|$ respectively, where the \mathcal{L} is the task loss and the C is the CLIP score[10]. Derivations of these criteria are in the supplementary. Experiments in Sec 4.3 and ablation studies in Sec 4.4 showed that our output loss pruning criterion significantly satisfies the additivity property and achieves the best performance among all the pruning criteria on different SDM models. Further, among the three pruning criteria we constructed, i.e., output loss, Δ task loss, and Δ CLIP score, for each model, the criteria with stronger additivity properties in Sec 4.3 achieved better pruning performance in Sec 4.4. This observation is justifiable since the one-shot layer pruning directly optimizes the surrogate objectives such as (6) rather than the original objective such as (2), optimizing those surrogate objectives that better approximate the original objectives can generally achieve better pruning performance. Based on the above observation and discussion, we can conclude that the effectiveness of our output loss criterion comes from its good additivity property.

3.3 Normalized Feature Distillation

In practice, we find that the pivotal objective for retraining is the feature loss \mathcal{L}_{FeatKD} . However, our further examinations revealed an imbalance issue in the previous feature distillation approaches employed in the retraining phase. As shown in Fig.3, both the L2-Norms of feature maps at the end of different stages and the values of different feature loss terms vary significantly. The same phenomenon shown in Fig.3 is observed on both SDXL and SDM-v1.5 under different pruning settings using either our layer pruning or handcrafted layer removal. The highest feature loss term is around 10000 times greater than the lowest one throughout the distillation process, and produces around 1000 times larger gradients, diluting the gradients of the numerically insignificant feature loss terms.



(a) Our 50% pruned SDXL. (b) Our 33% pruned SDM-v1.5

Figure 4: Unnormalized feature loss terms, i.e., $\|f_T^i - f_S^i\|_2^2$, of each stage using vanilla feature distillation or our normalized feature distillation, at the 15K-th iteration of retraining.

Since the feature maps with greater L2-Norms naturally tend to produce greater feature loss terms, the significant magnitude difference of different feature loss terms is attributed to two factors, i.e., at the end of different stages, the inherent dissimilarity of the feature maps between teacher and student varies, and the L2-Norm of the feature maps varies. The second factor aggravates the imbalance issue to a great extent.

Based on the above observations, simply adding up all the feature loss terms will cause the severe domination of a few feature loss terms over others, hindering the numerically insignificant feature loss terms from decreasing, leading to degraded performance. To this end, we proposed a simple yet effective re-weighting strategy for feature distillation to eliminate the second factor’s impact on the imbalance issue. We opt to leverage the L2-Norms of the teacher’s feature maps to re-weight the feature loss terms and adapt the feature distillation to our pruning scheme. The normalized feature loss is formulated as:

$$\mathcal{L}_{FeatKD-normed} = \sum_{i \in V} \mathbb{E}_{z,y,t} \alpha^i \|f_T^i(z_t, y, t) - f_S^i(z_t, y, t)\|_2^2 \quad (7)$$

$$\alpha^i = \frac{\sum_{j \in V} \|f_T^j(z_t, y, t)\|_2}{|V| \|f_T^i(z_t, y, t)\|_2},$$

where V is the set of stages where there are still residual layers or transformer layers remained after pruning, and $|V|$ is the size of set V . Hence, our overall retraining objective is:

$$\mathcal{L}_{all} = \mathcal{L}_{Task} + \lambda_{OutKD} \mathcal{L}_{OutKD} + \lambda_{FeatKD} \mathcal{L}_{FeatKD-normed}. \quad (8)$$

Without any hyperparameter tuning, we set λ_{OutKD} and λ_{FeatKD} to 1.

Discussions. We further investigated our method’s impact on different $\|f_T^i - f_S^i\|_2^2$ terms during retraining. As shown in Fig.4, by applying the normalized feature distillation, we observed significant declines of the $\|f_T^i - f_S^i\|_2^2$ terms at some stages with marginal increases elsewhere, proving that the dominance of a few feature loss terms over others is alleviated. Further ablation studies in Sec 4.5 showed that our method finally achieved great performance improvements.

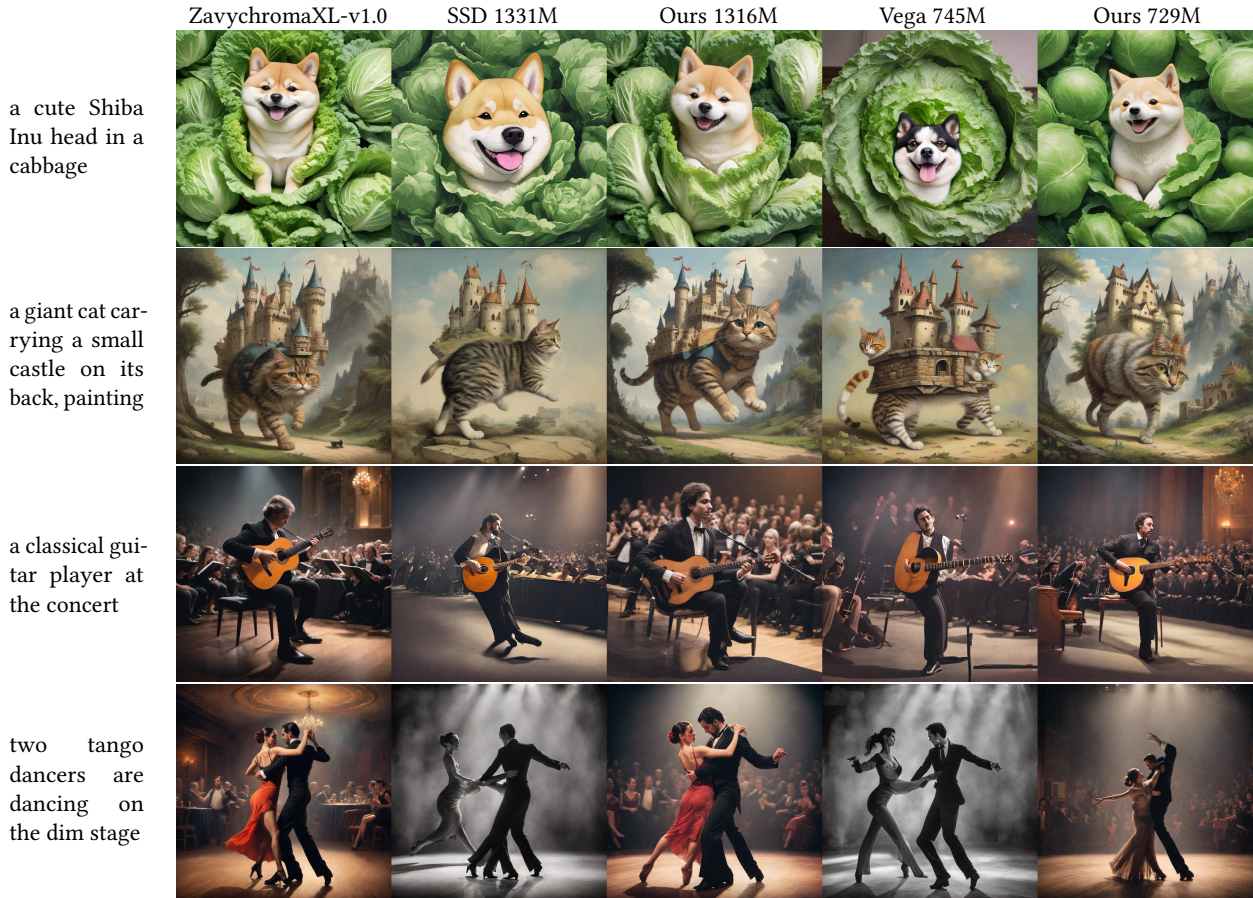


Figure 5: Visual comparison with SSD and Vega in DDIM 25 steps.

Method	Params of U-Net	HPS v2 \uparrow	PickScore \uparrow	ImageReward \uparrow	
Teacher: ZavychromaXL-v1.0[54]	Teacher	2567M	0.27968	0.2755	0.9950
	SSD[9]	1331M	0.27800	0.2529	0.9245
	Ours	1316M	0.27873	0.2644	0.9437
	Vega[9]	745M	0.27598	0.2412	0.7790
	Ours	729M	0.27758	0.2421	0.8210
Teacher: SDXL-Base-1.0[27]	Teacher	2567M	0.27213	0.2459	0.5187
	KOALA[19]	1161M	0.26963	0.2101	0.2604
	Ours	1142M	0.26968	0.2208	0.3281
	KOALA[19]	782M	0.26893	0.2045	0.2302
	Ours	764M	0.26913	0.2083	0.2603
Teacher: RealisticVision-v4.0[42]	Teacher	860M	0.27803	0.2399	0.7422
	BK-SDM[16, 40]	579M	0.27450	0.1999	0.5619
	Ours	578M	0.27575	0.2136	0.5807
	BK-SDM[16, 41]	323M	0.27030	0.1780	0.3142
	Ours	320M	0.27078	0.1782	0.3201

Table 1: Comparisons with the state-of-the-art methods.

4 EXPERIMENTS

4.1 Implementation

In this subsection, we mainly elaborate on the basic implementation settings. Further details are in the supplementary.

Model selection. Experiments in Sec 4.3, Sec 4.4 and Sec 4.5 are conducted on 512 \times 512 resolution for fast validation, using the ProtoVisionXL-v6.2.0[44] for SDXL model since the officially released SDXL-Base-1.0[27] renders anomalous images around

the 512×512 resolution, and using the officially released stable-diffusion-v1-5[32] for SDM-v1.5 model. For experiments in Sec 4.2, we use the same teacher model of each comparative method.

Dataset. For the calibration dataset used for pruning, we use a randomly sampled 1K subset of LAION-2B[39]. For the ablation studies in Sec 4.4 and Sec 4.5, we use a randomly sampled 0.34M subset of LAION-2B[39]. For the comparisons of the state-of-the-art methods in Sec.4.2, we use the same datasets of the comparative methods or turn to the datasets with lower quality and quantity if their reported datasets are hard to reproduce. The selections of datasets are detailed in the supplementary.

Evaluation metric. Although it has been a common practice to evaluate generative T2I models by FID[11] and CLIP score[10], recent studies[2, 17, 28, 48, 49] showed that these two metrics are poorly correlated with visual aesthetics and human preference. Therefore, we adopted 3 advanced metrics to evaluate the model’s comprehensive performance. We use HPS v2[48], PickScore[17], and ImageReward[50] to evaluate the general visual quality of the generated images and the text-image consistency. We calculate these 3 metrics on their own benchmark datasets, i.e., HPS v2 is calculated on its 3.2K benchmark dataset, ImageReward is calculated on a randomly sampled 3K subset of ImageRewardDB[51], and PickScore is calculated on a randomly sampled 3K subset of Pick-a-Pic v1[18].

4.2 Comparison with Other Methods

Up to now, there are three handcrafted layer removal methods for SDMs. KOALA[19], SSD and Vega[9] are on SDXL, and BK-SDM[16] can be applied on SDM-v1 or SDM-v2. We compare our LAPTOP-Diff with these three methods on the corresponding models. We use the SDXL-Base-1.0[27] for the comparison with KOALA 1.16B and 782M, the RealisticVision-v4.0[42] for the comparison with the more advanced BK-SDM[16] implementation by Segmind, i.e., 579M small-sd[40] and 323M tiny-sd[41]. For the comparison with 1.3B SSD[9] and 745M Vega[9], we only use one of the three teacher models they used in the multi-teacher distilling strategy, i.e., the ZavychromaXL-v1.0[54]. For all the evaluations of the comparative methods, we used their released model weights.

Tab.1 showed the comparison results with the state-of-the-art compressed SDM models. Our proposed LAPTOP-Diff achieved the most advanced performance. The visual comparisons with SSD[9] and Vega[9] are shown in Fig.5, and more visual comparisons with other methods are shown in the supplementary. We can observe that our method achieved better visual results on different prompts compared with other methods. Notably, it is also observed that our around 50% compressed SDXL model can achieve almost the same visual quality of the original model.

4.3 Validation of Additivity Property

Since the final surrogate objective (6) is the approximation of an upper bound of the original objective (2), it is necessary to examine the precision of the approximation. We simulate the values of the approximated criterion (6), and the real criterion (2), by choosing different m and R^m , covering the pruning ratio from 0% to 90%. We also conduct the same experiments on pruning criteria Δ task loss and Δ CLIP score. As shown in Fig.6, our output loss criterion

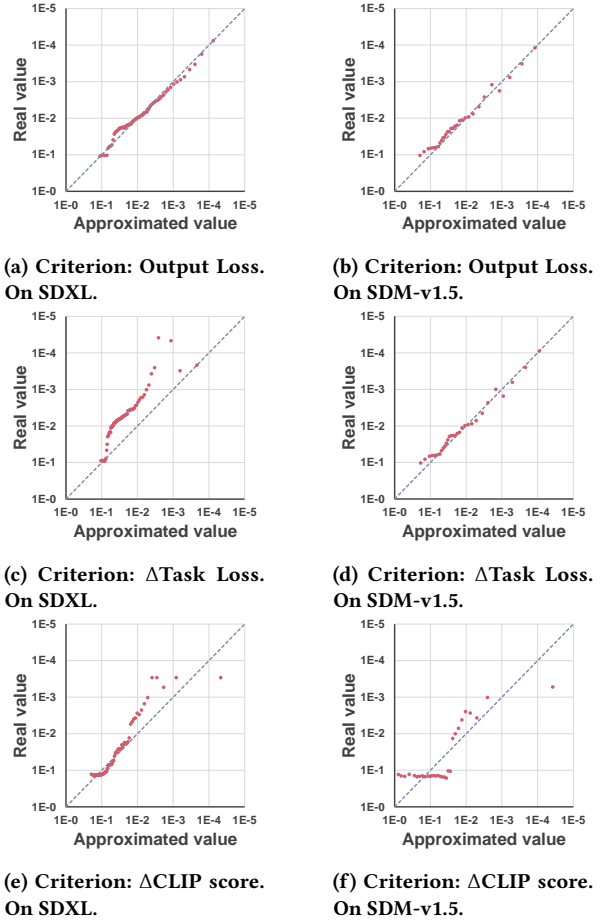


Figure 6: Validations of the additivity properties of different pruning criteria on SDXL and SDM-v1.5. Each point represents an observed value pair of the approximated criterion and the real criterion.

significantly satisfies the additivity property across different models even under an extreme pruning ratio of 90%, where almost all observation points are located near the identity line. Therefore, our final surrogate objective (6) is an excellent approximation of the original objective (2). On the other hand, other criteria fail to consistently satisfy the additivity property.

While our output loss criterion holds the strongest additivity property across different models, the Δ CLIP score holds the second strongest additivity on SDXL, and the Δ task loss holds the second strongest additivity on SDM-v1.5.

4.4 Ablation of Pruning Criteria

Experiments in Sec 4.3 showed that our output loss criterion significantly and consistently satisfies the additivity property while others fail. Furthermore, we evaluated the pruning performance using different pruning criteria including the pruning criteria we constructed and two baseline pruning criteria, i.e., the magnitude metric and the first-order Taylor-expansion of the loss function. We

Table 2: Comparisons of different pruning criteria. In addition, comparisons with handcrafted layer removal approaches are included.

	Method	HPS v2 \uparrow	PickScore \uparrow	ImageReward \uparrow
SDXL 50% pruned	Teacher	0.28085	0.2762	1.1769
	SSD[9]	0.27753	0.2445	0.8665
	Magnitude	0.26888	0.1980	0.4755
	Taylor	0.27925	0.2519	0.9290
	Δ Task Loss	0.27750	0.2493	0.9398
	Δ CLIP Score	0.27888	0.2537	0.9607
	Output Loss(Ours)	0.27928	0.2559	0.9844
SDM-v1.5 33% pruned	Teacher	0.27023	0.1965	0.1442
	BK-SDM[16]	0.25988	0.1148	-0.5698
	Magnitude	0.26160	0.1464	-0.3112
	Taylor	0.26318	0.1481	-0.3056
	Δ Task Loss	0.26390	0.1367	-0.3247
	Δ CLIP Score	0.26215	0.1351	-0.3715
	Output Loss(Ours)	0.26625	0.1517	-0.2189

Table 3: Comparisons between vanilla distillation and our normalized distillation.

	Method	HPS v2 \uparrow	PickScore \uparrow	ImageReward \uparrow
SDXL 50% pruned	Teacher	0.28085	0.2762	1.1769
	Vanilla KD	0.27933	0.2562	0.9852
	Normed KD(Ours)	0.27963	0.2564	1.0164
SDM-v1.5 33% pruned	Teacher	0.27023	0.1965	0.1442
	Vanilla KD	0.26780	0.1596	-0.0573
	Normed KD(Ours)	0.26810	0.1642	-0.0325

first prune the SDXL and SDM-v1.5 using different layer pruning criteria and then retrain the pruned network by vanilla distillation for the same training iterations. As shown in Tab.2, the output loss criterion attains the highest pruning performance among different pruning criteria on different models.

In addition to different pruning criteria, we also compared the layer pruning methods with handcrafted layer removal approaches. For the experiments on SDXL and SDM-v1.5, we use the same handcrafted layer removal settings of SSD[9] and BK-SDM[16] respectively. Results in Tab.2 showed that almost all the layer pruning approaches generally surpassed the handcrafted approaches except for the magnitude-based layer pruning is beaten by handcrafted approach SSD[9] on SDXL.

It is worth notice that, among the three pruning criteria we constructed, i.e., output loss, Δ task loss, and Δ CLIP score, while the output loss achieves the best performance across different models, the Δ CLIP score achieves the second best performance on SDXL, and the Δ task loss achieves the second best performance on SDM-v1.5, aligned with their ranks on additivity in Sec.4.3.

4.5 Ablation of Knowledge Distillation

We validate the effectiveness of our normalized feature distillation through ablation studies. We prune the SDXL and SDM-v1.5 by our one-shot layer pruning method and retrain the pruned network using vanilla distillation or our normalized distillation for the same training iterations. As shown in Tab.3, our method achieved great performance improvements on both SDXL and SDM-v1.5.

Table 4: Pruned U-Net architectures of SDXL and SDM-v1.5, using SDXL-Base-1.0[27] for SDXL at a total pruning ratio of 50% and stable-diffusion-v1-5[32] for SDM-v1.5 at a total pruning ratio of 33% as examples.

Model	Stage	# R_{ori}	# R_{prn}	# T_{ori}	# T_{prn}	P-Ratio
SDXL 50% pruned	Dn 1	2	0	0	0	0%
	Dn 2	2	0	4	0	0%
	Dn 3	2	0	20	18	83%
	Mid	2	0	10	8	67%
	Up 1	3	0	30	10	29%
	Up 2	3	0	6	0	0%
	Up 3	3	0	0	0	0%
	Dn Total	6	0	24	18	76%
	Up Total	9	0	36	10	26%
SDM-v1.5 33% pruned	Dn 1	2	0	2	0	0%
	Dn 2	2	0	2	0	0%
	Dn 3	2	0	2	2	50%
	Dn 4	2	2	0	0	100%
	Mid	2	2	1	1	100%
	Up 1	3	0	0	0	0%
	Up 2	3	0	3	1	13%
	Up 3	3	0	3	0	0%
	Up 4	3	0	3	0	0%
	Dn Total	8	2	6	2	53%
	Up Total	12	0	9	1	7%

R_{ori} : number of residual layers before pruning; # R_{prn} : number of pruned residual layers; # T_{ori} : number of transformer layers before pruning; # T_{prn} : number of pruned transformer layers; P-Ratio: pruning ratio in a stage.

4.6 Pruning Analysis

We analyzed the pruned architectures of SDXL’s U-Net at a pruning ratio of 50% and SDM-v1.5’s U-Net at a pruning ratio of 33% as examples. As Tab.4 shows, for both SDXL and SDM-v1.5, many layers in and near the Mid stage are considered less important and thus were pruned. This observation is consistent with the previous handcrafted layer removal approaches[9, 16, 19]. However, undiscovered by the previous handcrafted layer removal approaches, we observed that more layers are pruned at the Dn stages than the Up stages. For SDXL, we observed that 18 of the 30 layers were pruned in the Dn stages, but only 10 of the 45 were pruned in the Up stages. The same phenomenon is observed on SDM-v1.5 that 4 of the 14 layers were pruned in the Dn stages, while only 1 of the 21 were pruned in the Up stages. This observation is consistent with other studies[20, 26] that the Dn stage, i.e., the encoder of U-Net, is less important than the other parts of the U-Net.

5 CONCLUSION

In this work, we proposed the layer pruning and normalized distillation for compressing diffusion models(LAPTOP-Diff). We introduced the layer pruning approach to achieve automation, scalability, and better performance, and proposed an effective one-shot pruning criterion, i.e., the output loss criterion, whose effectiveness is ensured by its good additivity property. We further alleviated the imbalance issue of the previous distillation-based retraining using our proposed normalized feature distillation. Using the proposed LAPTOP-Diff, we compressed the SDMs for the most advanced performance.

REFERENCES

- [1] Daria Bakshandaeva Christoph Schuhmann Ksenia Ivanova Alex Shonenkov, Misha Konstantinov and Nadiia Klokova. 2023. *If by deepfloyd lab at stabilityai*. <https://huggingface.co/spaces/DeepFloyd/IF>
- [2] Eyal Betzalel, Coby Penso, Aviv Navon, and Ethan Fetaya. 2022. A study on the evaluation of generative models. *arXiv preprint arXiv:2206.10935* (2022).
- [3] Ollin Boer Bohan. 2023. *Sdxl-vae-fp16-fix*. <https://huggingface.co/madebyollin/sdxl-vae-fp16-fix>
- [4] Shi Chen and Qi Zhao. 2018. Shallowing deep networks: Layer-wise pruning based on feature representations. *TPAMI* (2018).
- [5] Yu-Hui Chen, Raman Sarokin, Juhyun Lee, Jiuqiang Tang, Chuo-Ling Chang, Andrei Kulik, and Matthias Grundmann. 2023. Speed is all you need: On-device acceleration of large diffusion models via gpu-aware optimizations. In *CVPR*.
- [6] Prafulla Dhariwal and Alexander Nichol. 2021. Diffusion models beat gans on image synthesis. In *NeurIPS*.
- [7] Sara Elkerdawy, Mostafa Elhoushi, Abhineet Singh, Hong Zhang, and Nilanjan Ray. 2020. To filter prune, or to layer prune, that is the question. In *ACCV*.
- [8] Gongfan Fang, Xinyin Ma, and Xinchao Wang. 2024. Structural pruning for diffusion models. In *NeurIPS*.
- [9] Yatharth Gupta, Vishnu V Jaddipal, Harish Prabhala, Sayak Paul, and Patrick Von Platen. 2024. Progressive Knowledge Distillation Of Stable Diffusion XL Using Layer Level Loss. *arXiv preprint arXiv:2401.02677* (2024).
- [10] Jack Hessel, Ari Holtzman, Maxwell Forbes, Ronan Le Bras, and Yejin Choi. 2021. CLIPScore: A Reference-free Evaluation Metric for Image Captioning. In *EMNLP*.
- [11] Martin Heusel, Hubert Ramsauer, Thomas Unterthiner, Bernhard Nessler, and Sepp Hochreiter. 2017. Gans trained by a two time-scale update rule converge to a local nash equilibrium. In *NeurIPS*.
- [12] Geoffrey Hinton, Oriol Vinyals, and Jeff Dean. 2014. Distilling the knowledge in a neural network. In *NeurIPS Workshop*.
- [13] Jonathan Ho, Ajay Jain, and Pieter Abbeel. 2020. Denoising diffusion probabilistic models. In *NeurIPS*.
- [14] Jonathan Ho and Tim Salimans. 2021. Classifier-Free Diffusion Guidance. In *NeurIPS 2021 Workshop on Deep Generative Models and Downstream Applications*.
- [15] Bo-Kyeong Kim, Geonmin Kim, Tae-Ho Kim, Thibault Castells, Shinkook Choi, Junho Shin, and Hyoung-Kyu Song. 2024. Shortened LLaMA: A Simple Depth Pruning for Large Language Models. *arXiv preprint arXiv:2402.02834* (2024).
- [16] Bo-Kyeong Kim, Hyoung-Kyu Song, Thibault Castells, and Shinkook Choi. 2023. On architectural compression of text-to-image diffusion models. *arXiv preprint arXiv:2305.15798* (2023).
- [17] Yuval Kirstain, Adam Polyak, Uriel Singer, Shahbuland Matiana, Joe Penna, and Omer Levy. 2023. Pick-a-pic: An open dataset of user preferences for text-to-image generation. In *NeurIPS*.
- [18] Yuval Kirstain, Adam Polyak, Uriel Singer, Shahbuland Matiana, Joe Penna, and Omer Levy. 2023. *pickapic_v1*. https://huggingface.co/datasets/yuvalkirstain/pickapic_v1
- [19] Youngwan Lee, Kwanyong Park, Yoorhim Cho, Yong-Ju Lee, and Sung Ju Hwang. 2023. KOALA: Self-attention matters in knowledge distillation of latent diffusion models for memory-efficient and fast image synthesis. *arXiv preprint arXiv:2312.04005* (2023).
- [20] Senmao Li, Taihang Hu, Fahad Shahbaz Khan, Linxuan Li, Shiqi Yang, Yaxing Wang, Ming-Ming Cheng, and Jian Yang. 2023. Faster diffusion: Rethinking the role of unet encoder in diffusion models. *arXiv preprint arXiv:2312.09608* (2023).
- [21] Xiuyu Li, Yijiang Liu, Long Lian, Huanrui Yang, Zhen Dong, Daniel Kang, Shanghang Zhang, and Kurt Keutzer. 2023. Q-diffusion: Quantizing diffusion models. In *ICCV*.
- [22] Xingchao Liu, Chengyue Gong, et al. 2022. Flow Straight and Fast: Learning to Generate and Transfer Data with Rectified Flow. In *ICLR*.
- [23] Cheng Lu, Yuhao Zhou, Fan Bao, Jianfei Chen, Chongxuan Li, and Jun Zhu. 2022. Dpm-solver: A fast ode solver for diffusion probabilistic model sampling in around 10 steps. In *NeurIPS*.
- [24] Cheng Lu, Yuhao Zhou, Fan Bao, Jianfei Chen, Chongxuan Li, and Jun Zhu. 2022. Dpm-solver++: Fast solver for guided sampling of diffusion probabilistic models. *arXiv preprint arXiv:2211.01095* (2022).
- [25] Simian Luo, Yiqin Tan, Longbo Huang, Jian Li, and Hang Zhao. 2023. Latent consistency models: Synthesizing high-resolution images with few-step inference. *arXiv preprint arXiv:2310.04378* (2023).
- [26] Xinyin Ma, Gongfan Fang, and Xinchao Wang. 2023. Deepcache: Accelerating diffusion models for free. *arXiv preprint arXiv:2312.00858* (2023).
- [27] Dustin Podell, Zion English, Kyle Lacey, Andreas Blattmann, Tim Dockhorn, Jonas Müller, Joe Penna, and Robin Rombach. 2023. *Stable-diffusion-xl-base-1.0*. <https://huggingface.co/stabilityai/stable-diffusion-xl-base-1.0>
- [28] Dustin Podell, Zion English, Kyle Lacey, Andreas Blattmann, Tim Dockhorn, Jonas Müller, Joe Penna, and Robin Rombach. 2024. SDXL: Improving Latent Diffusion Models for High-Resolution Image Synthesis. In *ICLR*.
- [29] Alec Radford, Jong Wook Kim, Chris Hallacy, Aditya Ramesh, Gabriel Goh, Sandhini Agarwal, Girish Sastry, Amanda Askell, Pamela Mishkin, Jack Clark, et al. 2021. Learning transferable visual models from natural language supervision. In *ICML*.
- [30] Aditya Ramesh, Mikhail Pavlov, Gabriel Goh, Scott Gray, Chelsea Voss, Alec Radford, Mark Chen, and Ilya Sutskever. 2021. Zero-shot text-to-image generation. In *ICML*.
- [31] Robin Rombach, Andreas Blattmann, Dominik Lorenz, Patrick Esser, and Björn Ommer. 2022. High-resolution image synthesis with latent diffusion models. In *CVPR*.
- [32] Robin Rombach, Andreas Blattmann, Dominik Lorenz, Patrick Esser, and Björn Ommer. 2022. *Stable-diffusion-v1-5*. <https://huggingface.co/runwayml/stable-diffusion-v1-5>
- [33] Adriana Romero, Nicolas Ballas, Samira Ebrahimi Kahou, Antoine Chassang, Carlo Gatta, and Yoshua Bengio. 2015. Fitnets: Hints for thin deep nets. In *ICLR*.
- [34] Chitwan Saharia, William Chan, Saurabh Saxena, Lala Li, Jay Whang, Emily L Denton, Kamyar Ghasemipour, Raphael Gontijo Lopes, Burcu Karagol Ayan, Tim Salimans, et al. 2022. Photorealistic text-to-image diffusion models with deep language understanding. In *NeurIPS*.
- [35] Tim Salimans and Jonathan Ho. 2022. Progressive Distillation for Fast Sampling of Diffusion Models. In *ICLR*.
- [36] Victor Sanh, Lysandre Debut, Julien Chaumond, and Thomas Wolf. 2019. DistilBERT, a distilled version of BERT: smaller, faster, cheaper and lighter. *arXiv preprint arXiv:1910.01108* (2019).
- [37] Axel Sauer, Dominik Lorenz, Andreas Blattmann, and Robin Rombach. 2023. Adversarial diffusion distillation. *arXiv preprint arXiv:2311.17042* (2023).
- [38] Christoph Schuhmann, Romain Beaumont, Richard Vencu, Cade Gordon, Ross Wightman, Mehdi Cherti, Theo Coombes, Aarush Katta, Clayton Mullis, Mitchell Wortsman, et al. 2022. *Laion-aesthetics v2 6+*. https://huggingface.co/datasets/ChristophSchuhmann/improved_aesthetics_6plus
- [39] Christoph Schuhmann, Romain Beaumont, Richard Vencu, Cade Gordon, Ross Wightman, Mehdi Cherti, Theo Coombes, Aarush Katta, Clayton Mullis, Mitchell Wortsman, et al. 2022. *Laion2B-en*. <https://huggingface.co/datasets/laion/laion2B-en>
- [40] Segmind. 2023. *Small-sd*. <https://huggingface.co/segmind/small-sd>
- [41] Segmind. 2023. *Tiny-sd*. <https://huggingface.co/segmind/tiny-sd>
- [42] SG_161222. 2023. *Realistic Vision*. <https://civitai.com/models/4201?modelVersionId=114367>
- [43] Yuzhang Shang, Zhihang Yuan, Bin Xie, Bingzhe Wu, and Yan Yan. 2023. Post-training quantization on diffusion models. In *CVPR*.
- [44] socialguitarist. 2023. *ProtoVision XL*. <https://civitai.com/models/125703?modelVersionId=172397>
- [45] Jiaming Song, Chenlin Meng, and Stefano Ermon. 2020. Denoising Diffusion Implicit Models. In *ICLR*.
- [46] Yang Song, Jascha Sohl-Dickstein, Diederik P Kingma, Abhishek Kumar, Stefano Ermon, and Ben Poole. 2021. Score-Based Generative Modeling through Stochastic Differential Equations. In *ICLR*.
- [47] Zhe Wang, Jie Lin, Xue Geng, Mohamed M Sabry Aly, and Vijay Chandrasekhar. 2022. RDO-Q: Extremely Fine-Grained Channel-Wise Quantization via Rate-Distortion Optimization. In *ECCV*.
- [48] Xiaoshi Wu, Yiming Hao, Keqiang Sun, Yixiong Chen, Feng Zhu, Rui Zhao, and Hongsheng Li. 2023. Human preference score v2: A solid benchmark for evaluating human preferences of text-to-image synthesis. *arXiv preprint arXiv:2306.09341* (2023).
- [49] Xiaoshi Wu, Keqiang Sun, Feng Zhu, Rui Zhao, and Hongsheng Li. 2023. Better aligning text-to-image models with human preference. In *ICCV*.
- [50] Jiazheng Xu, Xiao Liu, Yuchen Wu, Yuxuan Tong, Qinkai Li, Ming Ding, Jie Tang, and Yuxiao Dong. 2023. Imagereward: Learning and evaluating human preferences for text-to-image generation. In *NeurIPS*.
- [51] Jiazheng Xu, Xiao Liu, Yuchen Wu, Yuxuan Tong, Qinkai Li, Ming Ding, Jie Tang, and Yuxiao Dong. 2023. *ImageRewardDB*. <https://huggingface.co/datasets/THUDM/ImageRewardDB>
- [52] Kaixin Xu, Zhe Wang, Xue Geng, Min Wu, Xiaoli Li, and Weisi Lin. 2023. Efficient joint optimization of layer-adaptive weight pruning in deep neural networks. In *ICCV*.
- [53] Yanwu Xu, Yang Zhao, Zhisheng Xiao, and Tingbo Hou. 2023. Ufogen: You forward once large scale text-to-image generation via diffusion gans. *arXiv preprint arXiv:2311.09257* (2023).
- [54] Zavy. 2023. *ZavyChromaXL*. <https://civitai.com/models/119229/zavychromaxl>
- [55] Yang Zhao, Yanwu Xu, Zhisheng Xiao, and Tingbo Hou. 2023. MobileDiffusion: Subsecond Text-to-Image Generation on Mobile Devices. *arXiv preprint arXiv:2311.16567* (2023).

A SOLVING THE VARIANT OF 0-1 KNAPSACK PROBLEM

The optimization problem (6) in the main paper is a variant of 0-1 Knapsack problem. The $\mathbb{E}|\epsilon(l_i) - \epsilon_{ori}|_2^2$, $params(l_i)$ and P correspond to the value of the item, weight of the item and the knapsack capacity respectively. The objective is to find a subset of items that has a minimal total value while the total weight is no less than P . Similar to the original 0-1 Knapsack problem, this variant problem can also be solved by the dynamic programming algorithm or can be approximately solved by the greedy algorithm. We give the pseudocodes of the greedy algorithm and the dynamic programming algorithm as Algorithm.2 and Algorithm.3 respectively.

Algorithm 2 Solution to the variant of 0-1 Knapsack problem using greedy algorithm

Input: *values* array, *weights* array, the *knapsack_capacity* P
Output: An index set S of items that has a minimal total value while the total weight is no less than P

- 1: $n = \text{length}(\text{values})$
- 2: $S = \emptyset$
- 3: $k = 0$
- 4: $p = 0$ \triangleright current cumulative weight of the items in the bag
- 5: **while** $p < P$ **do**
- 6: $i = \text{index of the item that has the } k\text{-th smallest value}$
- 7: $p = p + \text{weights}[i]$
- 8: $S = S \cup \{i\}$ \triangleright the i -th item is in the bag
- 9: $k = k + 1$
- 10: **end while**
- 11: **return** S

B DERIVATIONS OF OTHER PRUNING CRITERIA

B.1 Derivation of Δ task loss

Let \mathcal{L}_{ori} denote the task loss of the original network, $\mathcal{L}(r_1, r_2, \dots, r_m)$ denote the task loss of the network where layers r_1, r_2, \dots, r_m are removed. We have the combinatorial optimization objective:

$$\begin{aligned} & \min_{r_1, \dots, r_m} \mathbb{E}|\mathcal{L}(r_1, \dots, r_m) - \mathcal{L}_{ori}| \\ \text{s.t. } & \{r_1, \dots, r_m\} \subset L^n, \sum_{i=1}^m \text{params}(r_i) \geq P. \end{aligned} \quad (9)$$

According to the triangle inequality, we have an upper bound of the objective (9):

$$\begin{aligned} & \mathbb{E}|\mathcal{L}(r_1, \dots, r_m) - \mathcal{L}_{ori}| \\ & \leq \mathbb{E}|\mathcal{L}(r_1) - \mathcal{L}_{ori}| \\ & \quad + \mathbb{E}|\mathcal{L}(r_1, r_2) - \mathcal{L}(r_1)| \\ & \quad + \dots \\ & \quad + \mathbb{E}|\mathcal{L}(r_1, \dots, r_m) - \mathcal{L}(r_1, \dots, r_{m-1})|. \end{aligned} \quad (10)$$

Algorithm 3 Solution to the variant of 0-1 Knapsack problem using dynamic programming algorithm

Input: *values* array, *weights* array, the *knapsack_capacity* P
Output: An index set S of items that has a minimal total value while the total weight is no less than P

Search for a minimal objective value:

- 1: $n = \text{length}(\text{values})$
- 2: $dp = \text{zero array of shape } (n, P + 1)$
- 3: **for** $j = 0$ to P **do**
- 4: **if** $\text{weight}[0] < j$ **then** $dp[0, j] = \text{infinite}$
- 5: **else** $dp[0, j] = \text{value}[0]$
- 6: **end for**
- 7: **for** $i = 0$ to $n - 1$ **do**
- 8: **for** $j = P$ to 0 **do**
- 9: **if** $\text{weight}[i] < j$ **then** $dp[i, j] = \min(dp[i-1, j], dp[i-1, j - \text{weight}[i]] + \text{value}[i])$
- 10: **else** $dp[i, j] = \min(dp[i-1, j], \text{value}[i])$
- 11: **if** $\text{sum}(\text{weight}[:i+1]) < j$ **then** $dp[i, j] = \text{infinity}$
- 12: **end for**
- 13: **end for**

Get the solution to the minimal objective:

- 14: $S = \emptyset$
- 15: **def** DFS(i, j):
- 16: **if** $j = 0$ **then Return**
- 17: **if** $i = 0$ **and** $\text{weight}[0] \geq j$ **then**
- 18: $S = S \cup \{i\}$ \triangleright the i -th item is in the bag
- 19: **Return**
- 20: **if** $\text{weight}[i] < j$ **then**
- 21: **if** $dp[i, j] = dp[i-1, j - \text{weight}[i]] + \text{value}[i]$ **then**
- 22: $S = S \cup \{i\}$ \triangleright the i -th item is in the bag
- 23: DFS($i-1, j - \text{weight}[i]$) \triangleright depth-first search
- 24: **else** DFS($i-1, j$) \triangleright depth-first search
- 25: **else**
- 26: **if** $dp[i, j] = \text{value}[i]$ **then**
- 27: $S = S \cup \{i\}$ \triangleright the i -th item is in the bag
- 28: **Return**
- 29: **else** DFS($i-1, j$) \triangleright depth-first search
- 30: DFS($n-1, P$) \triangleright start the recursion
- 31: **return** S

Similar to the assumption (5) in the main paper, we have the assumption:

$$\begin{aligned} & \mathbb{E}|\mathcal{L}(r_1, \dots, r_{i-1}, r_i) - \mathcal{L}(r_1, \dots, r_{i-1})| \\ & \approx \mathbb{E}|\mathcal{L}(r_1, \dots, r_{i-2}, r_i) - \mathcal{L}(r_1, \dots, r_{i-2})| \\ & \approx \dots \\ & \approx \mathbb{E}|\mathcal{L}(r_1, r_i) - \epsilon(r_1)| \\ & \approx \mathbb{E}|\mathcal{L}(r_i) - \mathcal{L}_{ori}|. \end{aligned} \quad (11)$$

However, different from assumption (5), the assumption (11) may not be satisfied well across different models according to the Validation of Additivity Property section in the main paper.

Section	Model	Dataset	Resolution	Total Batch Size	Iterations	Learning Rate
Sec 4.2	ZavychromaXL v1.0[54] for the comparison with SSD[9] and Vega[9]	8M LAION Aesthetics V2 6+[38]	1024×1024		100K and 240K	1E-5
	SDXL-Base-1.0[27] for the comparison with KOALA[19]	8M LAION Aesthetics V2 6+[38]	1024×1024	128	125K	1E-5
	RealisticVision-v4.0[42] for the comparison with BK-SDM[16]	0.34M subset of LAION-2B[39]	512×512		120K	1E-4
Sec 4.3	ProtoVisionXL-v6.2.0[44] for SDXL stable-diffusion-v1-5[32] for SDM-v1.5	1K subset of LAION-2B[39]	512×512	-	-	-
Sec 4.4	ProtoVisionXL-v6.2.0[44] for SDXL	0.34M subset of LAION-2B[39]	512×512	512	15K	1E-5
	stable-diffusion-v1-5[32] for SDM-v1.5		128	12K		
Sec 4.5	ProtoVisionXL-v6.2.0[44] for SDXL	0.34M subset of LAION-2B[39]	512×512	512	30K	1E-5
	stable-diffusion-v1-5[32] for SDM-v1.5		128	60K		

Table 5: Implementation details of the experiments in each section of the main paper.

With the approximation (11) and the upper bound (10), we have the surrogate objective:

$$\min_{r_1, \dots, r_m} \sum_{i=1}^m \mathbb{E} |\mathcal{L}(r_i) - \mathcal{L}_{ori}| \quad (12)$$

$$s.t. \{r_1, \dots, r_m\} \subset L^n, \sum_{i=1}^m \text{params}(r_i) \geq P.$$

Here, $\mathbb{E} |\mathcal{L}(r_i) - \mathcal{L}_{ori}|$ is the Δ task loss between the original network and the network where only layer r_i is removed.

B.2 Derivation of Δ CLIP score

Let C_{ori} denote the CLIP score of the original network, $C(r_1, r_2, \dots, r_m)$ denote the CLIP score of the network where layers r_1, r_2, \dots, r_m are removed. The form of the derivation of Δ CLIP score is the same as the derivation of Δ task loss. Simply replace the \mathcal{L} and \mathcal{L}_{ori} appear in the Supplementary.B.1 with C and C_{ori} respectively, and we can get the final objective:

$$\min_{r_1, \dots, r_m} \sum_{i=1}^m \mathbb{E} |C(r_i) - C_{ori}| \quad (13)$$

$$s.t. \{r_1, \dots, r_m\} \subset L^n, \sum_{i=1}^m \text{params}(r_i) \geq P.$$

Here, $\mathbb{E} |C(r_i) - C_{ori}|$ is the Δ CLIP score between the original network and the network where only layer r_i is removed.

C FURTHER IMPLEMENTATION DETAILS

In addition to the basic implementation information in the main paper, further details are summarised in Tab.5.

All the experiments are conducted with the Diffusers library using FP16 precision. We use the same VAEs and text encoders of the original SDXL and SDM-v1.5, except for the sdxl-vae-fp16-fix[3] VAE checkpoint for SDXL model since the SDXL’s original VAE is incompatible with FP16 precision computation.

For training, we use the AdamW optimizer with constant learning rates shown in Tab.5 while other hyperparameters of the optimizer maintain default.

For inference, we use the DDIM scheduler[45] for SDXL, and DPM-Solver++[23, 24] for SDM-v1.5, all with 25 denoising steps and the default 7.5 classifier-free guidance scale[14].

D LATENCY ANALYSIS

Tab.6 shows the latencies of the original models and our compressed models. Our 50% and 72% compressed SDXL U-Nets are 33% and

Resolution	Model	U-Net(1)	U-Net(25)	Whole
1024 × 1024	SDXL 2567M	0.113s	2.83s	3.25s
	Ours 1316M	0.076s	1.90s	2.33s
	Ours 729M	0.059s	1.48s	1.89s
512 × 512	SDM-v1.5 860M	0.028s	0.70s	0.77s
	Ours 578M	0.023s	0.58s	0.68s
	Ours 320M	0.019s	0.48s	0.56s

Table 6: Latency analysis of the original models and our compressed models. U-Net(1) for the latency of a single denoising step, U-Net(25) for 25 denoising steps, and Whole for the whole generating process of an image in 25 denoising steps, including text encoder, U-Net, and VAE decoder computations. Latencies are measured on NVIDIA A100 GPU.

48% faster than the original U-Net, and our 33% and 63% compressed SDM-v1.5 U-Nets are 17% and 31% faster than the original U-Net.

E VISUAL COMPARISONS WITH OTHER METHODS

The visual comparisons with KOALA[19] and BK-SDM[16] are shown in Fig.7 and Fig.8, respectively. We can observe that our method achieved better visual results on different prompts compared with other methods. Notably, it is also observed that our 55% compressed SDXL-Base-1.0 and 33% compressed RealisticVision-v4.0 can achieve almost the same visual qualities of the original models.



Figure 7: Visual comparison with KOALA in DDIM 25 steps.

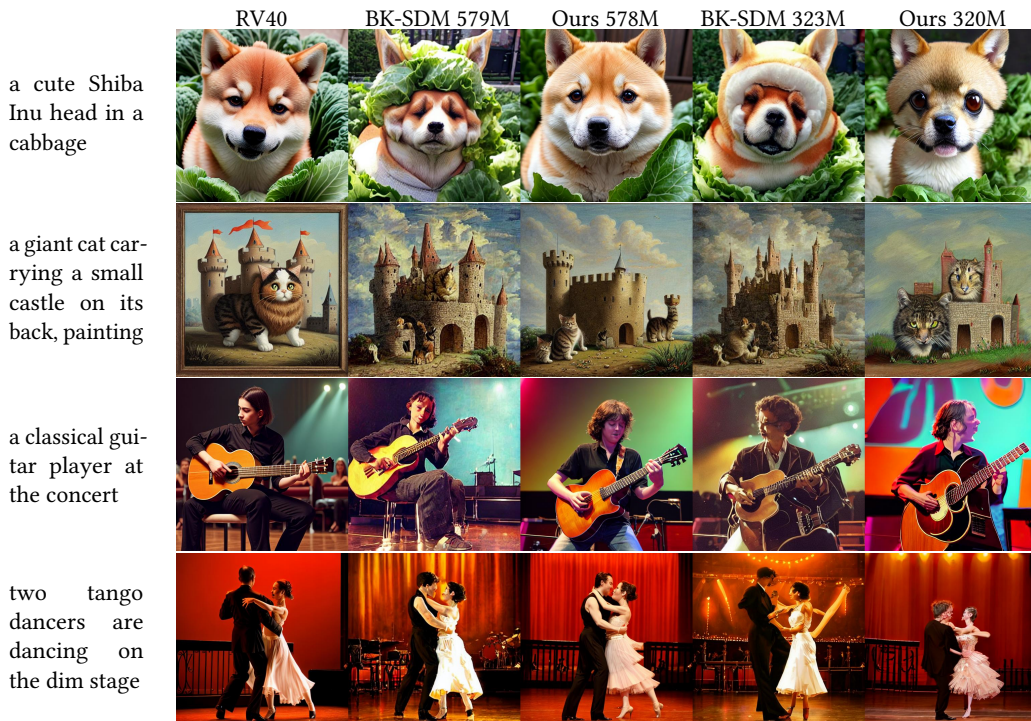


Figure 8: Visual comparison with BK-SDM, implemented using RealisticVision-v4.0(RV40) as teacher, in DPM++ 25 steps.